A black phosphorus-graphite hybrid as a Li-ion regulator enabling stable lithium deposition

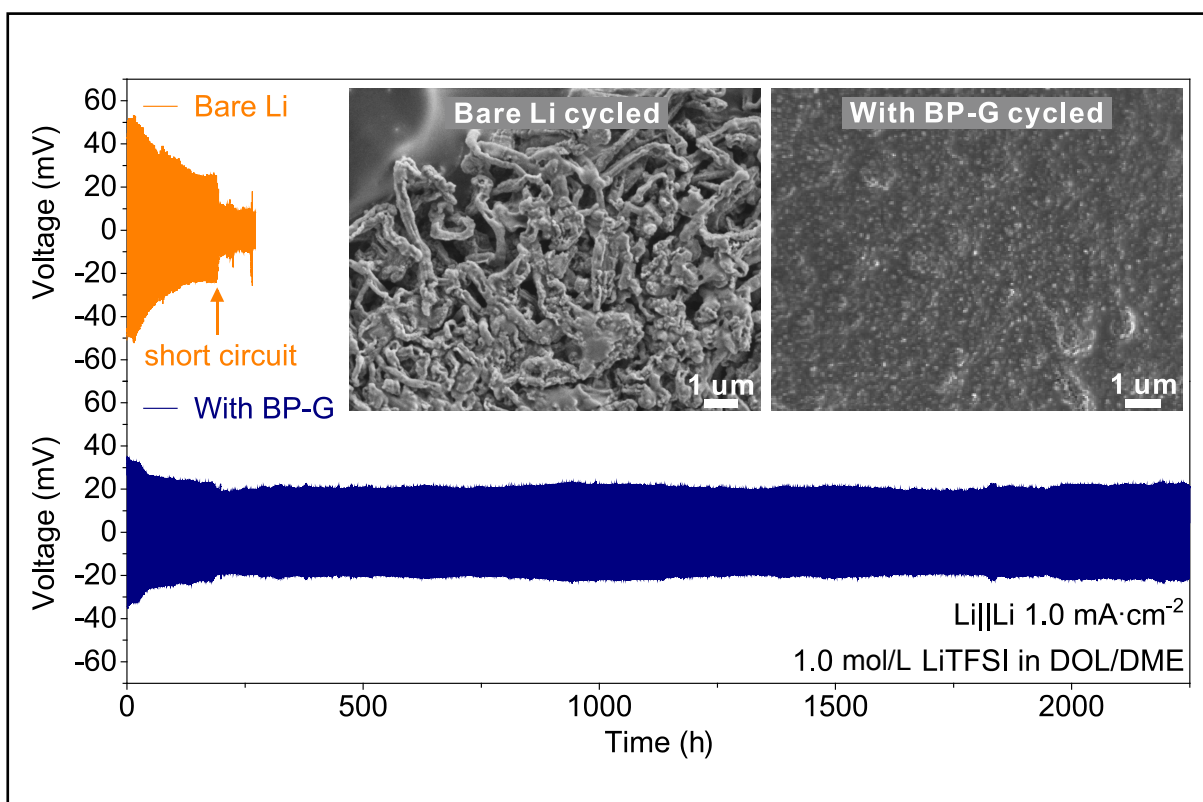Huanyu Xie[*], Chaonan Wang[*], En Zhou, Hongchang Jin [✉], and Hengxing Ji [✉]

Hefei National Research Center for Physical Sciences at the Microscale and Department of Applied Chemistry, University of Science and Technology of China, Hefei 230026, China

* These authors contributed equally to this work
[✉]Correspondence: Hongchang Jin, E-mail: jhckimi@ustc.edu.cn; Hengxing Ji, E-mail: jihengx@ustc.edu.cn

Graphical abstract

A black phosphorus-graphite hybrid acts as the Li-ion regulator, enabling stable lithium deposition.

Public summary

- The hybrid of black phosphorus-graphite (BP-G) is introduced to serve as an artificial protective layer of a Li metal anode.

- The utilization of Li metal achieves > 98.5% for over 500 cycles in Li‖Cu half cells and the life span maintains over 2000 h in Li‖Li symmetric cells with a low voltage hysteresis of 50 mV.

- The LFP‖Li full cell with BP-G Li-ion regulator offers a high specific capacity (162 mA·h·g^{-1} with 81% capacity retention until the 300th cycle).

A black phosphorus-graphite hybrid as a Li-ion regulator enabling stable lithium deposition

Huanyu Xie[*], Chaonan Wang[*], En Zhou, Hongchang Jin ✉, and Hengxing Ji ✉

Hefei National Research Center for Physical Sciences at the Microscale and Department of Applied Chemistry, University of Science and Technology of China, Hefei 230026, China

* These authors contributed equally to this work
✉Correspondence: Hongchang Jin, E-mail: jhckimi@ustc.edu.cn; Hengxing Ji, E-mail: jihengx@ustc.edu.cn

Abstract: Lithium (Li) metal anodes have been regarded as the most promising candidates for high energy density secondary lithium batteries due to their high specific capacity and low redox potential. However, the issues of Li dendrites caused by nonuniform lithium deposition during battery cycling severely hinder the practical applications of Li metal anodes. Herein, a hybrid of black phosphorus-graphite (BP-G) is introduced to serve as an artificial protective layer for the Li metal anode. The two-dimensional few-layer BP, which is lithophilic, combined with the high electronic conductive graphite can act as a regulator to adjust the migration of Li ions, delivering a uniform and stable lithium deposition. As the growth of lithium dendrites is inhibited, the utilization of Li metal achieves > 98.5% for over 500 cycles in Li∥Cu half cells, and the life span is maintained over 2000 h in Li∥Li symmetric cells with a low voltage hysteresis of 50 mV. Moreover, the LiFePO$_4$∥Li full cell with a BP-G Li-ion regulator presents significantly better specific capacity and cycling stability than that with the bare Li metal anode. Therefore, the introduction of the BP-G Li-ion regulator is demonstrated to be an effective approach to enable stable lithium deposition for rechargeable Li metal batteries.

Keywords: lithium metal deposition; black phosphorus; graphite

CLC number: TM912; TB33   **Document code:** A

1   Introduction

Due to the high theoretical capacity (3860 mA·h·g^{-1}) and low redox potential (−3.04 V, vs standard hydrogen electrode, SHE), Lithium (Li) metal is considered an ideal anode material for high energy density batteries[1, 2]. However, the stable plating/stripping of Li metal tends to be impeded by side reactions between Li metal and electrolyte, and lithium dendrites grow uncontrollably, which leads to low Coulombic efficiency (CE), poor cycling stability, and heavy safety risks[3−6]. In practical lithium metal batteries (LMBs), the solid electrolyte interphase (SEI) is of vital importance to avoid the continuous side reactions between the Li metal and electrolyte and thus regulate the nucleation and uniform deposition of lithium metal[7]. Nevertheless, the naturally formed SEI with an inhomogeneous composition on the Li metal surface is mechanically fragile and results in continuous fracture and recombination under large volume changes, which lead to a nonuniform SEI structure[8]. Furthermore, the nonuniform SEI induces lithium dendrite growth during the Li deposition process, which further leads to SEI cracking and accelerates electrolyte consumption. During the subsequent Li-stripping process, parts of the lithium dendrites may be disconnected from the electrode, resulting in dead lithium, which also causes the depletion of fresh lithium by side reactions with the electrolyte. Therefore, stabilizing the SEI structure and regulating the Li-ion distribution on the lithium surface are important to improve the cycling stability of Li metal anodes.

The growth of dendritic lithium will not only accelerate the consumption of active materials but also increase the risk of short circuits, greatly shortening the life span of the battery[9]. To date, great efforts have been devoted to modifying or replacing electrolyte-derived SEIs, including adjusting electrolyte components[10], developing high-modulus solid-state electrolytes[11], and designing artificial protective layers (e.g., two-dimensional materials and polymers)[12]. To alleviate the problems mentioned above, one strategy is to introduce an artificial protective layer onto the lithium metal anode, regulating the migration behavior and distribution of Li ions. Practically, as the uneven flux of solvated Li ions reaches the lithium metal surface, it is rather important to regulate Li-ion migration by hindering the migration of anions and preventing the solvent sheath from contacting the lithium metal anode[13], which is a fundamental way to suppress dendritic lithium growth and prolong the battery life span. Herein, we introduce a black phosphorus-graphite hybrid as a Li-ion regulator enabling stable lithium deposition.

Black phosphorus (BP) is composed of phosphorene layers stacked in puckered subplanes through the weak interactions of van der Waals force[14]. The crystal lattice of BP is composed of diatomic layers, and each layer is composed of a tortuous chain of phosphorus (P) atoms. BP is a semiconductor with a density of 2.70 g·cm^{-3} and a Mons' hardness scale of 2.

Moreover, the diffusion coefficient of Li ions within a phosphorene monolayer in the zigzag direction is estimated to be ~100 times faster than that of the graphene layer at room temperature[15]. The mixture of BP and graphite (G) was ball milled to fabricate a hybrid of black phosphorus-graphite (BP-G). Due to the affinity and diffusion ability of black phosphorus for Li ions and the high electronic conductivity introduced by graphite, the artificial protective layer of the BP-G hybrid can induce uniform deposition of Li ions on the Li metal surface and increase the transference number for Li ions at the same time, reducing the side reactions of anions and solvent molecules with lithium metal. With the BP-G Li-ion regulator, the Coulombic efficiency and cycling life of the lithium metal anode can be greatly improved.

2 Experimental

2.1 Materials and characterization

For battery tests, 1.0 mol·L^{-1} Li bis(trifluoromethane-sulfonyl)imide (LiTFSI) dissolved in 1,3-dioxolane/1,2-dimethoxyethane (DOL/DME, 1 : 1 in volume) with 2.0 wt% lithium nitrate (LiNO$_3$) additive was used as the electrolyte. Bulk BP was synthesized from red phosphorus by the chemical vapor transport (CVT) method and further exfoliated into few-layer BP flakes. The BP-G hybrid was fabricated by ball milling a mixture of few-layer BP flakes and commercial graphite at a mass ratio of 1 : 1.

The structure of the BP-G hybrid was examined by Raman spectra, which were recorded at room temperature with a 532 nm excitation laser. Transmission electron microscopy (TEM, JEM-2100F), high-resolution transmission electron microscopy (HRTEM) images and elemental mappings were acquired to observe the morphology, lattice structure and composition of the BP-G hybrid. The morphologies of the bare Li and (BP-G)/Li metal were characterized by scanning electron microscopy (SEM, Gemini SEM 500 instrument).

2.2 Preparation of (BP-G)/Li metal anodes

The hybrid of BP-G was first dispersed in N-methyl-2-pyrrolidone (NMP) solvent at a concentration of 1 mg·mL^{-1}, and then the dispersion was stirred for 30 min in an argon-filled glove box before uniformly coating the surface of Li foils with a certain amount of BP-G. The modified Li foils were then dried naturally in a glove box to obtain the (BP-G)/Li metal anodes.

### 2.3 Electrochemical measurements

The cathodes were prepared by mixing commercial LiFePO$_4$ (LFP) powder with Ketjen black and PVDF at a mass ratio of 84 : 8 : 8, and then the slurry was cast onto aluminum (Al) foil by a doctor blade. The mass loading of LFP is 4.5 mg·cm^{-2}, and the thickness of the Li metal foil is approximately 60 μm. For each coin cell, 30 μL electrolyte was added for electrochemical tests. The galvanostatic charge/discharge tests and short circuit tests were conducted by a Land battery test system. Electrochemical impedance spectroscopy (EIS) measurements (0.1–1×10^5 Hz) and Tafel curves were conducted on Princeton Applied Research analytical equipment.

2.4 Li-ion transference number measurements

The Li-ion transference number (t) was measured in the Li‖Li symmetric cells following a previously reported method. The value of t was obtained by EIS (0.1–1×10^5 Hz, amplitude of 10 mV) before (R_0) and after (R_s) direct current polarization with a constant voltage of 5 mV (ΔV). The polarization process took over 1×10^4 s to reach a steady state, and the current values at the initial (I_0) and steady states (I_s) were recorded. The transference number was then calculated by the following equation:

$$t = \frac{I_s(\Delta V - I_0 R_0)}{I_0(\Delta V - I_s R_s)}. \tag{1}$$

The EIS results were fitted according to the equivalent circuit below by ZSimpWin software.
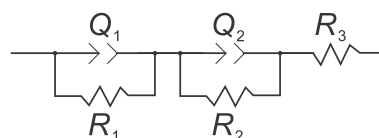
Specifically, R_1 and R_2 represent the interface resistances (R_{ct}) in Li‖Li symmetric cells, and R_3 represents the bulk resistance. Q_1 and Q_2 represent the constant phase elements.

3 Results and discussion

3.1 Structure of the BP-G hybrid

The Raman spectrum shows three intense bands of the A$_g^1$, B$_{2g}$, and A$_g^2$ vibration modes of BP at 363, 440, and 467 cm^{-1}, respectively (Fig. 1a). The Raman bands at 1330 and 1590 cm^{-1} are attributed to the D and G bands of graphite, respectively[16]. The micromorphology of BP-G was characterized by transmission electron microscopy (TEM), and the TEM image of the hybrid shows the particle morphology of BP-G (Fig. 1b). Moreover, the high-resolution transmission electron microscopy (HRTEM) image shows a detailed view of the edge of graphite, and a lattice spacing of 3.4 Å can be measured, corresponding to the d-spacing across the basal planes of graphite. The lattice fringes with a d-spacing of 4.2 Å can be ascribed to the (100) lattice plane of the BP crystal (Fig. 1c). Furthermore, TEM elemental mappings show that P and C are uniformly distributed in the BP-G particle (Fig. 1d–f). These results indicate that the intrinsic structures of BP and G are well preserved in the BP-G hybrid, and these two elements are also well mixed and uniformly dispersed after ball milling.

Subsequently, the BP-G hybrid is uniformly modified to the surface of the bare Li foil to form an artificial protective layer. Under scanning electron microscope (SEM) observation, (BP-G)/Li foil shows a smooth surface (Fig. 1g), which is similar to the bare Li foil (Fig. 1h), suggesting that BP-G can be coated on Li foil uniformly. In addition, the cross-section image of (BP-G)/Li foil was also acquired by SEM, showing that the BP-G layer fits tightly on the surface of Li foil with a thickness of 5 μm. Therefore, the BP-G protective layer was successfully introduced to the surface of the lithium metal anode, accompanied by a uniformly flat surface and
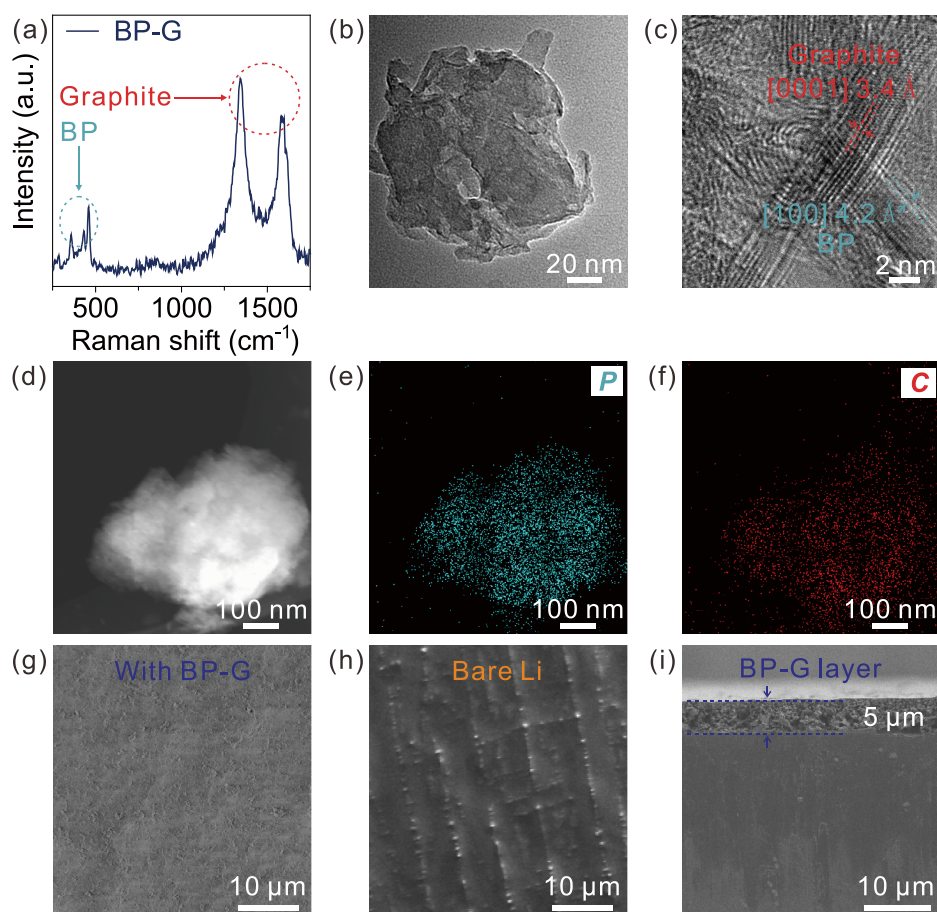
Fig. 1. Structure characterization. (a) Raman spectra, (b) TEM, and (c) HRTEM images of the BP-G hybrid. (d–f) TEM elemental mapping images of the BP-G hybrid. SEM images of the (g) (BP-G)/Li surface, (h) bare Li metal, and (i) cross section of (BP-G)/Li.

a suitable thickness.

3.2 Li-ion transport

To our knowledge, solvated Li ions with an uneven concentration distribution reaching the Li metal surface are the main cause for the growth of Li dendrites[17]. Moreover, the transportation of Li ions in the electrolyte and SEI, which is much slower than the transportation of electrons in the electrodes, is usually the rate-determining step of lithium deposition. Therefore, regulating the migration of Li ions reaching the lithium metal surface is an effective strategy to suppress the growth of Li dendrites and prolong the battery life span[18]. Generally, the transportation behaviors of Li ions were studied by Li‖Li symmetric cells and Li‖Cu half cells, which consisted of Li metal foils as the working electrodes with or without a BP-G protective layer.

To validate the interface charge transfer advantage with the BP-G Li-ion regulator, Tafel curves of the Li‖Li symmetric cells were recorded, and the kinetic advantage of (BP-G)/Li foil can be demonstrated by the exchange current density (Fig. 2a)[19]. The higher exchange current density with BP-G (0.64 mA·cm^{-2}) than the bare Li foil (0.52 mA·cm^{-2}) enables a faster charge transfer at the interface of the electrolyte and lithium metal anode, which can suppress the parasitic reactions and further provide stable lithium deposition. Likewise, the continuous growth of lithium dendrites, which is mainly caused by the uneven Li metal deposition, would finally lead to the short circuit of the battery, resulting in a sharp voltage drop of the cell[20]. Then, short-circuit tests were performed with Li‖Cu half cells, during which the lithium metal was continuously plated on the Cu electrode surface until a short circuit appeared. As shown in Fig. 2b, the cell assembled with the (BP-G)/Li foil can maintain a continuous lithium deposition for over 125 h at a current density of 1.0 mA·cm^{-2}, whereas the voltage of the cell assembled with a bare Li foil fluctuates and suddenly drops from −55 mV to −4 mV after 78 h, indicating a short circuit of the cell.

Furthermore, the Li-ion transference numbers (t) for the modified and bare lithium metal anodes were measured by a direct current polarization method[21]. The transference number is defined as the fraction of the charge carried by a certain species of ion to the total charge in the electrolyte, which is mainly determined by the ion mobility. Electrochemical impedance spectroscopy (EIS) measurements of the cells assembled with (BP-G)/Li and bare Li foils exhibit very close internal resistances (4.2–5.1 Ω), indicating that the introduction of the BP-G protective layer hardly affects the internal resistance of the battery. With the charge transfer resistances (R_{ct}) before and after polarization (Fig. 2c, d) and the polarization current values at the initial and stable states (Fig. 2e, f), the Li-ion transference numbers of the bare Li and (BP-G)/Li anodes can be calculated as 0.37 and 0.62, respectively. The significant improvement in Li-ion transference numbers with the BP-G regulator can be ascribed to the affinity for Li ions
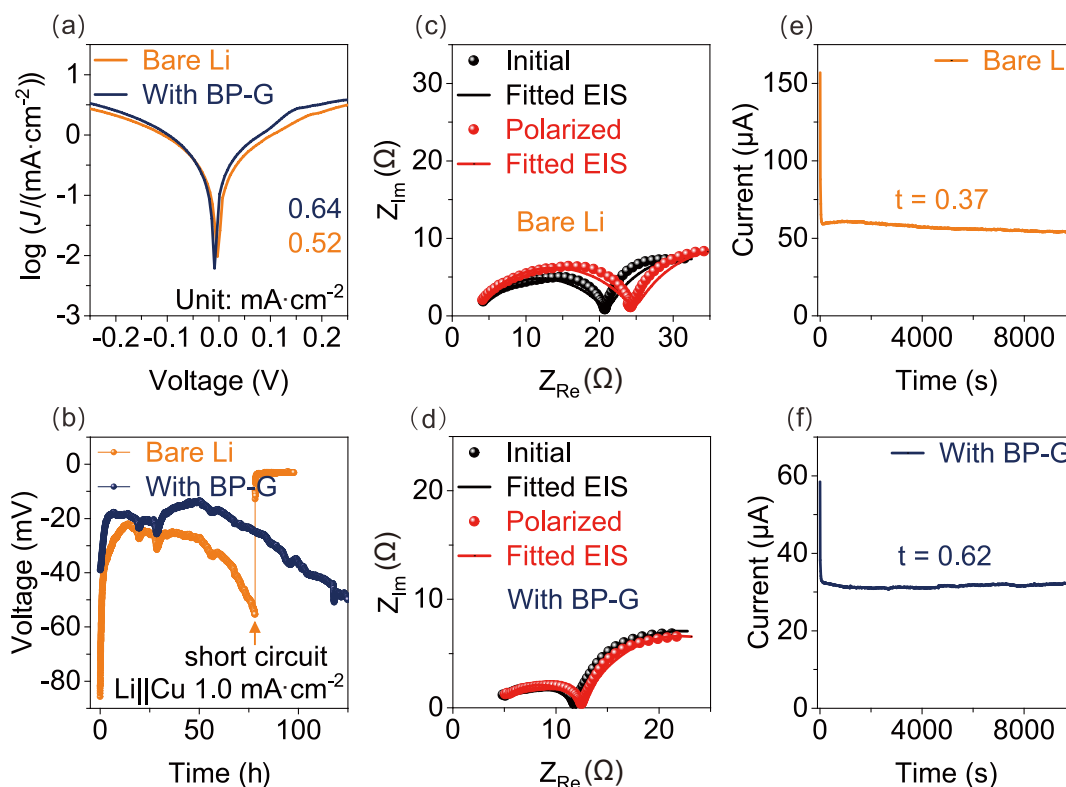
Fig. 2. Li-ion transportation behaviors. (a) Tafel curves of the Li‖Li symmetric cells with or without the BP-G layer to evaluate the exchange current densities. (b) Short circuit tests of Li‖Cu half cells with bare Li or (BP-G)/Li metal anodes at 1.0 mA·cm^{-2}. Nyquist plots of Li‖Li symmetric cells before and after polarization with the (c) bare Li and (d) (BP-G)/Li metal anodes; the corresponding direct current polarization curves of the (e) bare Li and (f) (BP-G)/Li metal anodes.

and induced deposition by BP. The increased Li-ion transference number is also helpful to exclude the side reactions that involve the anions or the solvent molecules, such as the formation of SEI. Furthermore, since Sand's time, defined as the time lithium dendrites start to grow, is inversely proportional to the square of the anionic mobility, the increased Li-ion transference number accompanied by a decreased anionic mobility can lead to a larger Sand's time, rendering the stable deposition of lithium metal anodes. These results proved that the BP-G protective layer can act as a Li-ion regulator, enabling stable lithium deposition.

3.3 Electrochemical performance

To measure the improvement of Coulombic efficiency and long-term cycling performance with a BP-G protective layer, the applications of the (BP-G)/Li and bare Li metal anodes were investigated by Li‖Cu half cells, Li‖Li symmetrical cells, and LFP‖Li full cells.

For a lithium metal battery, CE shows the amount of irreversible consumption of lithium metal during the repeated cycles due to the formation of SEI films and dead Li. Hence, the quite low Coulombic efficiency of the bare Li metal anodes will directly affect the cycling life span of a practical battery[22]. To measure the values of CE, a fixed amount of lithium metal is electroplated on a copper foil during cycling, and then the plated lithium metal is stripped back to the lithium metal anode. Coulombic efficiency is defined as the ratio of the stripped and plated lithium metal. The BP-G-modified Li metal anode exhibits a more stable cycling performance

with enhanced CE and prolonged cycling life in an ether-based DOL/DME electrolyte than those with bare Li metal (Fig. 3a). The cell with the BP-G protective layer has a high CE above 98.5% for over 500 cycles. The low CE for the initial several cycles can be ascribed to the side reactions between lithium metal and BP-G or electrolyte, such as the formation of SEI. In comparison, although the CE of a bare Li metal anode can remain quite high compared to that of the (BP-G)/Li anode in the first 100 cycles, it starts to decline and fluctuate rapidly, indicating that the consumption of lithium metal resulted from the electrolyte depletion and growth of dendritic Li. The charge/discharge curves at the 50th (Fig. 3b) and 100th (Fig. 3c) cycles also exhibit an enhancement in electrochemical deposition with a higher CE and smaller polarization.

The long-term cycling performance was further investigated by Li‖Li symmetric cells in a DOL/DME electrolyte. During the cycling tests, Li ions are transported back and forth between the two Li metal electrodes with or without the BP-G protective layer. The current density and areal capacity are set to be 1.0 mA·cm^{-2} and 1.0 mA·h·cm^{-2}, respectively. The voltage profiles are shown in Fig. 3d. The voltage hysteresis of the Li‖Li symmetric cell with the bare Li metal anode (orange line) is initially as large as 100 mV, then gradually decreases within an activation stage, and it suddenly drops from 42 to 20 mV after 190 h of cycling, indicating the short circuit inside the cell resulting from the gradually accumulated dendritic Li. In comparison, the cell with the (BP-G)/Li anode (blue line) renders a constant and stable voltage profile
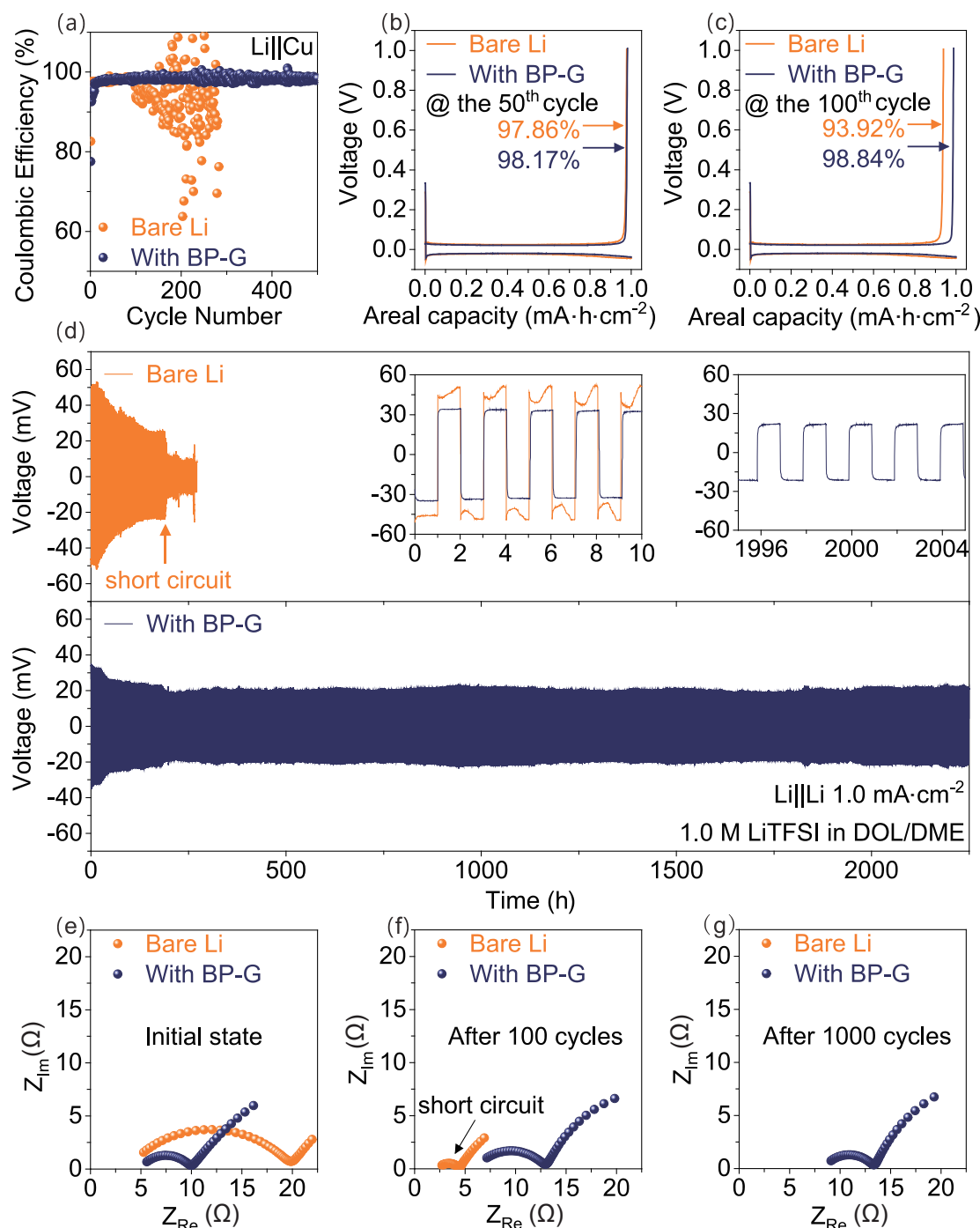
Fig. 3. Electrochemical performances of Li‖Cu half cells and Li‖Li symmetric cells. (a) The variation of CE values in Li‖Cu cells with the bare Li or (BP-G)/Li metal anodes at the current density of 1.0 mA·cm⁻² and areal capacity of 1.0 mA·h·cm⁻². The corresponding charge/discharge curves at the (b) 50th and (c) 100th cycles. (d) Voltage profiles of Li‖Li symmetric cells with the bare Li (orange line) and (BP-G)/Li (blue line) metal anodes at a current density of 1.0 mA·cm⁻² and an areal capacity of 1.0 mA·h·cm⁻². The insets show the corresponding enlarged voltage profiles at different cycling stages. Impedance spectra of Li‖Li symmetric cells with the bare Li or (BP-G)/Li metal anodes at (e) the initial state and the end of the (f) 100th and (g) 1000th cycles.

of ∼ 50 mV for over 2000 h, which is much more extended to that of the bare Li metal anode, suggesting a uniform and stable lithium deposition interface. In addition, the insets show the corresponding enlarged voltage profiles at different cycling stages, from which it can be seen that the voltage profiles with the BP-G Li-ion regulator show a much more stable plating/stripping voltage than that of the bare Li metal anode.

The electrochemical impedances of Li‖Li symmetrical cells

from the abovementioned long-term cycling tests were measured at the initial state (Fig. 3e) and the end of the 100th (Fig. 3f) and 1000th (Fig. 3g) cycles. The results were analyzed through equivalent circuit model fitting to provide quantitative information, where the impedance spectra of Li‖Li symmetric cells can be decoupled into charge transfer resistances (R_{ct}, interfacial resistance) and bulk resistances (R_{bulk}, internal resistance). At the initial state, the charge transfer resist-

ance of the (BP-G)/Li anode is much lower than that of the bare Li metal anode (4.8 Ω vs 14.9 Ω), indicating a smaller barrier for the electroplating of Li ions. In addition, the bulk resistances with the BP-G Li-ion regulator are also more stable, with fitted R_{bulk} values ranging from 5.2 Ω at the initial state to 8.7 Ω after 1000 cycles, suggesting the inhibited growth of lithium dendrites and little electrolyte consumption. However, as the short circuit occurs in the battery, the R_{ct} and R_{bulk} values of the bare Li metal anode exhibit a sharp decrease after 100 cycles, indicating unstable Li plating and stripping behaviors with the bare Li metal anode.

The electrochemical performances of LFP‖Li full cells with the bare Li and (BP-G)/Li anodes were investigated to demonstrate the practical application of the BP-G Li-ion regulator. During cycling, the cell with the (BP-G)/Li anode exhibits a higher specific capacity and an excellent capacity retention compared with that of the bare Li metal anode (Fig. 4a). The initial specific capacity of 162 mA·h·g⁻¹ is reached at 1.0 C with a BP-G Li-ion regulator, which maintains excellent cycling performance of 81% capacity retention (131 mA·h·g⁻¹) until the 300th cycle. However, although the initial specific capacity of the bare Li metal anode can reach 161 mA·h·g⁻¹, it decays rapidly during cycling, and the Coulombic efficiencies are also greatly reduced after 220 cycles. The charge/discharge curves at the 10th and 300th cycles are recorded and shown in Fig. 4b. The cell with the BP-G Li-ion regulator renders a smaller polarization than that of the bare Li metal, which can be attributed to the reduced formation of Li dendrites and electrolyte consumption. Furthermore, the morphology of lithium metal anodes is regarded as direct

evidence of stable deposition[17]. Hence, SEM images of the bare Li and (BP-G)/Li anodes after cycling in LFP‖Li full cells were collected for comparison. Obviously, sharp dendrites are observed on the bare Li metal surface accompanying the decreased specific capacity (Fig. 4c). In contrast, a smooth surface of the (BP-G)/Li anode is maintained after cycling (Fig. 4d), proving the inhibited growth of Li dendrites with the BP-G Li-ion regulator. These results further confirmed the stable cycling stability and prolonged cycle life contributed by the BP-G hybrid, which is consistent with the electrochemical performances.

4 Conclusions

In conclusion, the hybrid of BP-G can act as a Li-ion regulator, rendering stable lithium deposition by enhancing the Li-ion transference number and alleviating the deposition barrier for Li-ions, resulting from the uniformly distributed lithophilic sites by BP-G, which facilitate the transport and homogeneous dispersion of Li-ions. Therefore, the deposition of Li metal in the cell with the (BP-G)/Li anode is dense and smooth. As a consequence of the multiple beneficial properties of the BP-G protective layer, the suppressed growth of Li dendrites and dead Li on the anode enables a remarkable enhancement in the utilization of Li metal (CE > 98.5% for over 500 cycles), life span (> 2000 h), and low voltage hysteresis (~ 50 mV). Furthermore, the LFP‖Li full cell with a BP-G Li-ion regulator offers a high specific capacity (162 mA·h·g⁻¹ with 81% capacity retention until the 300th cycle). Therefore, the BP-G Li-ion regulator substantially improves the performance of Li metal anodes, enabling an advanced design
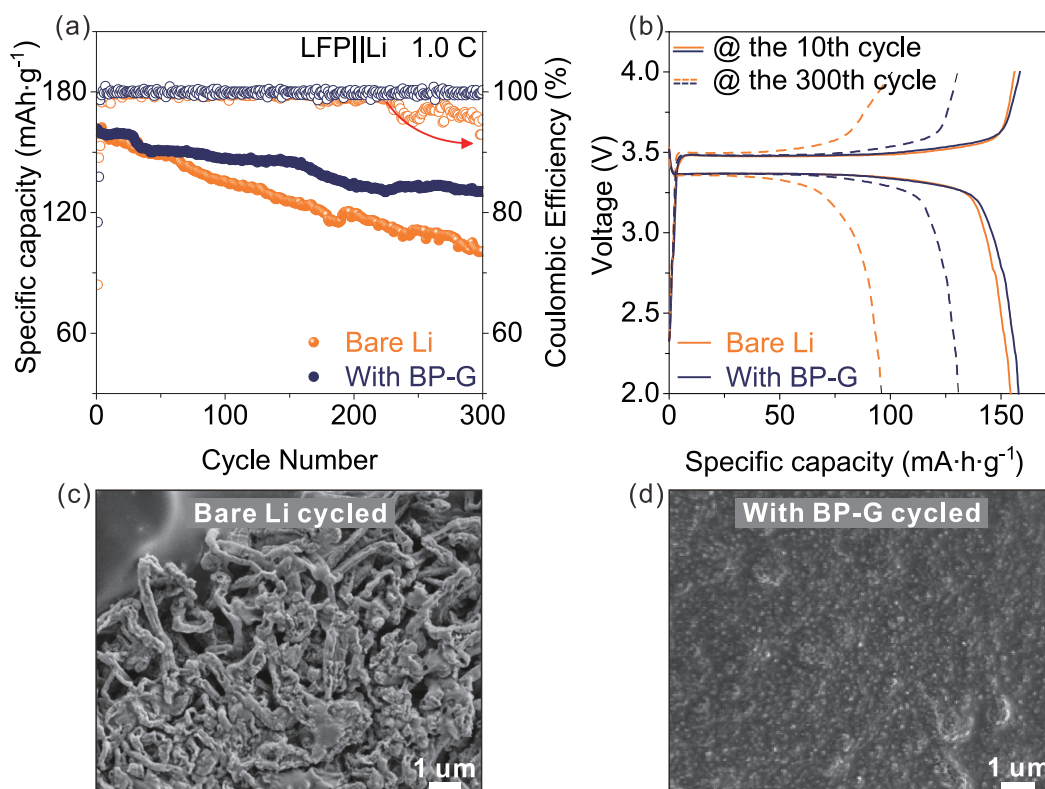

Fig. 4. Electrochemical performances of LFP‖Li full cells. (a) Variation in specific capacity retention with cycle numbers at 1.0 C. (b) Charge/discharge voltage profiles of the 10th and 300th cycles. Morphologies of lithium metal anodes after 300 cycles with the (c) bare Li or (d) (BP-G)/Li metal anodes.

strategy for advanced lithium metal batteries with high energy density.

Acknowledgements

Conflict of interest

The authors declare that they have no conflict of interest.

Biographies

Huanyu Xie is currently a postdoctoral fellow at the University of Science and Technology of China (USTC). He received his Ph.D. degree in Materials Science and Engineering from USTC in 2022 under the supervision of Prof. Hengxing Ji. He then joined Prof. Hengxing Ji's group as a postdoctoral fellow in June 2022. His scientific interests include the protection and design of the anodes of lithium secondary batteries.

Chaonan Wang is presently a Ph.D. student in the Department of Applied Chemistry, University of Science and Technology of China (USTC). He received his bachelor's degree from the School of Chemistry and Materials Science, USTC, in 2020. His research mainly focuses on the application of 2D materials in energy storage devices.

Hongchang Jin received his Ph.D. degree from the University of Science and Technology of China (USTC) in 2019 and is currently a postdoctoral researcher in USTC. His research mainly focuses on phosphorus-based anode materials for fast charging lithium-ion batteries.

Hengxing Ji has been a Professor at the School of Chemistry and Materials Science, University of Science and Technology of China (USTC), since 2013. He received his B.S. degree in 2003 from USTC and his Ph.D. degree in 2008 from the Institute of Chemistry, Chinese Academy of Sciences, under the supervision of Prof. Li-Jun Wan. He then joined Leibniz Institute for Solid State and Materials Research Dresden in 2008, working with Prof. Oliver G. Schmidt as a Humboldt research fellow before moving to the University of Texas at Austin in 2010, working with Prof. Rodney S. Ruoff as a postdoctoral researcher. His research interests include low-dimensional carbon nanostructures and micro/nanomaterials and devices for energy conversion and storage.

References

[1] Sheng L, Wang Q, Liu X, et al. Suppressing electrolyte-lithium metal reactivity via Li(+)-desolvation in uniform nano-porous separator. *Nat. Commun.,* **2022**, *13* (1): 172.

[2] Winter M, Barnett B, Xu K. Before Li ion batteries. *Chem. Rev.,* **2018**, *118* (23): 11433–11456.

[3] Wang M, Emre A E, Kim J Y, et al. Multifactorial engineering of biomimetic membranes for batteries with multiple high-performance parameters. *Nat. Commun.,* **2022**, *13* (1): 278.

[4] Yao Y X, Zhang X Q, Li B Q, et al. A compact inorganic layer for robust anode protection in lithium‐sulfur batteries. *InfoMat,* **2020**, *2* (2): 379–388.

[5] Li J, Kong Z, Liu X, et al. Strategies to anode protection in lithium metal battery: A review. *InfoMat,* **2021**, *3* (12): 1333–1363.

[6] Han Z, Zhang C, Lin Q, et al. A protective layer for lithium metal anode: Why and how. *Small Methods,* **2021**, *5* (4): 2001035.

[7] Ye Y, Zhao Y, Zhao T, et al. An Antipulverization and high-continuity lithium metal anode for high-energy lithium batteries. *Adv. Mater.,* **2021**, *33* (49): 2105029.

[8] Gao Y, Rojas T, Wang K, et al. Low-temperature and high-rate-charging lithium metal batteries enabled by an electrochemically active monolayer-regulated interface. *Nat. Energy,* **2020**, *5* (7): 534–542.

[9] Wang Q, Yang C, Yang J, et al. Dendrite-free lithium deposition via a superfilling mechanism for high-performance Li-metal batteries. *Adv. Mater.,* **2019**, *31* (41): 1903248.

[10] Zheng J, Yan P, Mei D, et al. Highly stable operation of lithium metal batteries enabled by the formation of a transient high-concentration electrolyte layer. *Adv. Energy Mater.,* **2016**, *6* (8): 1502151.

[11] Huang M, Yao Z, Yang Q, et al. Consecutive nucleation and confinement modulation towards Li plating in seeded capsules for durable Li-metal batteries. *Angew. Chem. Int. Ed.,* **2021**, *60* (25): 14040–14050.

[12] Xu Y, Zhou Y, Li T, et al. Multifunctional covalent organic frameworks for high capacity and dendrite-free lithium metal batteries. *Energy Stor. Mater.,* **2020**, *25*: 334–341.

[13] Chang Z, Qiao Y, Yang H, et al. Sustainable lithium-metal battery achieved by a safe electrolyte based on recyclable and low-cost molecular sieve. *Angew. Chem. Int. Ed.,* **2021**, *60* (28): 15572–15581.

[14] Lange S, Schmidt P, Nilges T. Au$_3$SnP$_7$@ black phosphorus: An easy access to black phosphorus. *Inorg. Chem.,* **2007**, *46* (10): 4028–4035.

[15] Sun J, Sun Y, Pasta M, et al. Entrapment of polysulfides by a black-phosphorus-modified separator for lithium-sulfur batteries. *Adv. Mater.,* **2016**, *28* (44): 9797–9803.

[16] Jin H, Xin S, Chuang C, et al. Black phosphorus composites with engineered interfaces for high-rate high-capacity lithium storage. *Science,* **2020**, *370*: 192–197.

[17] Zhao C Z, Chen P Y, Zhang R, et al. An ion redistributor for dendrite-free lithium metal anodes. *Sci. Adv.,* **2018**, *4* (11): eaat3446.

[18] Chang Z, Qiao Y, Deng H, et al. A liquid electrolyte with de-solvated lithium ions for lithium-metal battery. *Joule,* **2020**, *4* (8): 1776–1789.

[19] He X, Jin S, Miao L, et al. A 3D hydroxylated MXene/carbon nanotubes composite as a scaffold for dendrite-free sodium-metal electrodes. *Angew. Chem. Int. Ed.,* **2020**, *59* (38): 16705–16711.

[20] Xie H, Hao Q, Jin H, et al. Redistribution of Li-ions using covalent organic frameworks towards dendrite-free lithium anodes: A mechanism based on a Galton Board. *Sci. China Chem.,* **2020**, *63* (9): 1306–1314.

[21] He Y, Chang Z, Wu S, et al. Simultaneously inhibiting lithium dendrites growth and polysulfides shuttle by a flexible MOF-based membrane in Li-S batteries. *Adv. Energy Mater.,* **2018**, *8* (34): 1802130.

[22] Tang X, Zhou D, Li P, et al. MXene-based dendrite-free potassium metal batteries. *Adv. Mater.,* **2020**, *32* (4): 1906739.